Materials Science-Poland, *Vol. 27*, *No. 3*, *2009*

Modification of gold nanoparticle surfaces with pyrenedisulfide in ligand-protected exchange reactions*

P. UZNAŃSKI**, J. KURJATA, E. BRYSZEWSKA

Centre for Molecular and Macromolecular Studies, Polish Academy of Sciences,
Sienkiewicza 112, 90-363 Łódź, Poland

We provide a study of ligand place-exchange reaction on Au nanoparticles. Nanoparticles of the dimensions of 7–9 nm were fabricated by high-temperature anhydrous route in the presence of primary aliphatic amine. The advantage of weak coordination to gold, through the nonbonding electrons of the amino group, was to use in an exchange of an initial protective ligand. Therefore, among other stabilizing agents, photoactive dialkyldisulfide molecules functionalized with fluorescent pyrene moieties were attached. The photophysical properties of such a stabilized gold system were investigated during place-exchange reaction. Fluorescence studies show that the excimeric band, characteristic of bispyrene, disappears in the spectrum after binding to the gold NPs, indicating that pyrene molecules are adsorbed separately on the surface. Efficient quenching of monomeric emission suggests that deactivation of the fluorescent excited state occurs through a radiationless transition, probably a charge transfer one, formed due to prior electron transfer from pyrene moiety to gold. Kinetics of chemisorption of pyrene disulfide and its desorption in the presence of thiols was also studied, revealing that both processes comprise a fast and a slow component with an overall rate higher for the desorption.

Key words: *gold nanoparticles; ligand exchange; pyrene; functionalization*

1. Introduction

Since the important paper by Brust et al. [1], extensive studies have been carried out on ligand-protected noble metal particles. These investigations include alternative methods for the syntheses of gold nanoparticles (NPs) [2], introduction of chemical functional groups to the particle surface [3], in-place exchange reaction of an original ligand [4–8], controllable NPs arrangements [9], etc. We have recently described a new anhydrous method for the synthesis of gold NPs from triphosphinogold oxon-

---

*The paper presented at the 11th International Conference on Electrical and Related Properties of Organic Solids (ERPOS-11), July 13–17, 2008, Piechowice, Poland.

**Corresponding author, e-mail: puznansk@cbmm.lodz.pl

ium salt $[O(AuPPh_3)_3]BF_4$ in the presence of amine [10]. This precursor was found to be a versatile gold atom source in mesitylene in the presence of primary amine which, apart from playing a stabilizing role, takes part in the reduction of gold(I) atom. One of the advantages of this route is that primary amines containing long aliphatic chains would be easily exchanged for other functionalized ligands. It is a fundamentally and technologically important aspect as the composition of the stabilizing shell of parent nanoparticles can be modified, hence allowing controllable synthesis of stable nanoparticles with different chemical properties such as solubility or reactivity. Functionalized nanoparticles maintain the dimensions of the original particles and exhibit enhanced resistance to decomposition and aggregation.

For a better understanding of the properties of nanoparticles obtained from gold oxonium salt, we have studied a colloidal stabilization by various ligands and dynamics of ligand exchange on the nanoparticle surface. HDA-protected particles were functionalized by various capping agents being not exposed to the reaction conditions under which the metal particles themselves are formed. We have also employed fluorescence of pyrene as a probe for electronic interactions of the surface-bound organic group with the metal core, due to its special photophysical properties exemplified by a structured emission band sensitive to the polarity of its environment and concentration dependent excimer emission [11].

Luminescence properties of gold–chromophore systems attract increasing attention because of their potential in applications. However, only a few examples of studies have been reported on arrangements, interactions, and photophysical behaviour of ligands with gold core using the fluorescence probe method [7, 8, 12–15]. We have to emphasize that the molecular probe method, apparently, is extremely helpful in studies of ligand motion on nanoparticle surfaces [6, 16].

2. Experimental

Materials. 1-Hexadecanethiol (HDT), 1-Hexadecylamine (HDA), 1,8-diaminooctane (diAO), and tetraoctylammonium bromide (TOABr) purchased from Aldrich were used as received. Dichloromethane and toluene, prior to use, were distilled over CaH_2. Gold oxonium salt $[O(AuPPh_3)_3]BF_4$ was prepared according to previously published methods [17]. Symmetric bispyrene disulfide (diSPy) was synthesized by pyrene bromoalkylation according to the method described in [4], followed by thiol substitution *via* the procedure worked out in [12]. The corresponding thiol was converted to disulphide using the oxidation of thiol, as proposed in [18]. ^{1}H NMR ($CDCl_3$, 200Mz) δ 8.27 (d, 1H, J = 9,27 Hz); 8.01 (m, 7H); 7.85 (d, 1H, J = 6.83 Hz); 3.32 (t, 2H, J = 7,53 Hz), 2.67 (t, 2H, J = 7.30 Hz); 1.85 (m, 2H); 1.65 (m, 2H), 1.27 (m, 14H). All other reagents and solvents were used as-received from Aldrich.

Characterization techniques. ^{1}H NMR spectra were recorded with a Bruker Avance AV 200 MHz spectrometer. Absorption measurements were made on a Hew-

lett Packard HP8453 photodiode array instrument and fluorescence spectra were collected with a Perkin-Elmer LS50 luminescence spectrometer in a 1 cm quartz cell.

Synthesis. Gold nanoparticles stabilized with hexadecylamine (HDA) AuNPs-HDA were synthesized in a monophasic system which employs triphosphinogold oxonium salt $[O(AuPPh_3)_3]BF_4$ as a gold atom source (Scheme 1). With a large excess of amine in mesitylene, oxonium salt transforms to gold ammonium salt, which at elevated temperatures and under aerated conditions decomposes into gold neutral atoms and phosphine–gold clusters. Initially, HDA plays the role of a reducing agent but finally the excess amine molecules act as a stabilizing ligand, tightly covering the NPs surface. This propriety of AuNPs-HDA nanoparticles was exploited in in-place ligand exchange reactions. The average size of the NPs is in the range of 7–9 nm. Details of the synthesis and characterization of AuNPs-HDA are given in our previous communication [10].

$$(Ph_3PAu)_3OBF_4^- \xrightarrow[-H_2O]{+\ HDA} (Ph_3PAu)_3NBF_4^- \xrightarrow[-RNH_3BF_4]{+\ 3HDA} 3\ (RNHAuPPh_3) \qquad R = (-C_{16}H_{33})$$

$$3\ (RNHAuPPh_3) \xrightarrow{+\ H_2O,\ \Delta T} Au^0 + Ph_3P{=}O + (Ph_3P)_nAu + NH_2R$$

Scheme 1. Synthesis of hexadecylamine protected gold nanoparticles

Disulfide coated gold nanoparticles AuNPs-diSPy were synthesized by a ligand exchange reaction, with the parent AuNPs-HDA particles at an excess of disulfide. A solution of 5 mg of AuNPs-HDA in toluene (2 cm^3) was mixed with a dichloromethane solution of 2.5 mg of pyrenedisulfide. The reaction mixture was stirred rapidly at 45 °C for 3 h. Upon completion of the ligand exchange, the solvent was removed under a rotary evaporator. Crude NPs were dissolved in a minimum amount of toluene and purified by repeated precipitation with ethanol (3×6 cm^3). The dark blue powder was further characterized by spectroscopic techniques. We have found that the reaction time for diSPy is longer than that for HDT molecules. The obtained NPs were redispersed in dichloromethane for further studies.

3. Results and discussion

3.1. Binding of diamine and ammonium salt to HDA-protected gold nanoparticles

The binding of aliphatic diamine and charged aliphatic ammonium salt to HDA protected gold nanoparticles was studied by UV-vis spectroscopy, taking advantage of the enhanced optical absorption associated with surface plasmon resonance of gold. The plasmon peak of colloidal nanoparticles results from resonant excitations of collective oscillations of conductive electrons in metal with incident light. The position of

this peak depends on the particle size, shape, solvent, and the distance between particles. A solution of the parent AuNPs-HDA nanoparticles was mixed with equivalent amounts of 1,8-diaminooctane or tetraoctylammonium bromide. The temporal evolution of the plasmon band of NPs in CH_2Cl_2 after the addition of diAOc or TOABr is presented in Fig. 1.

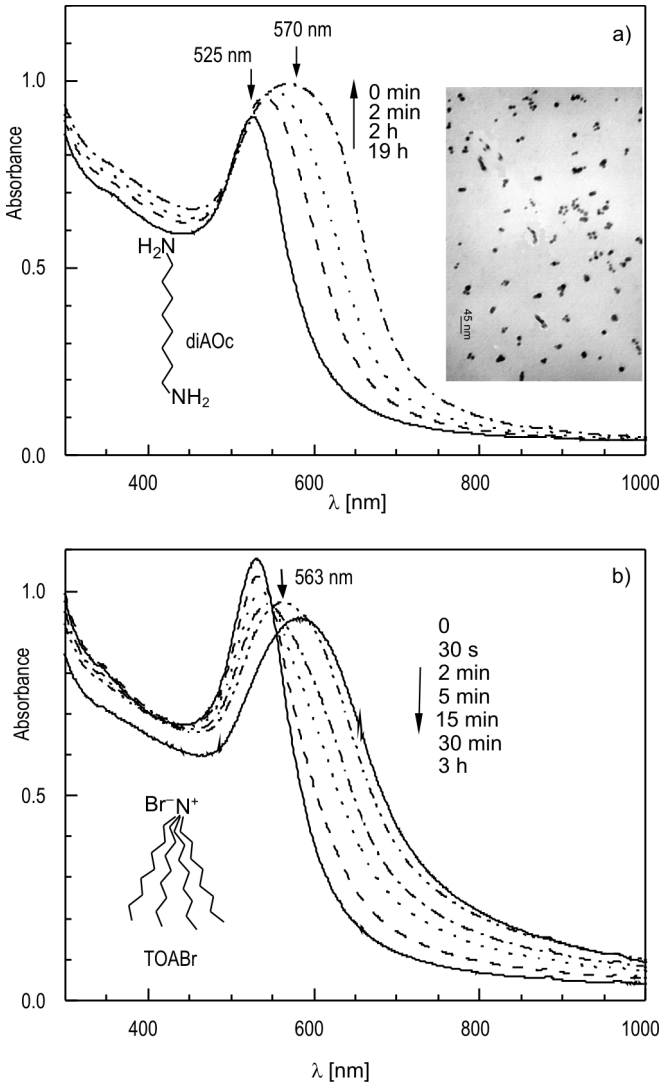

Fig. 1. Temporal evolution of the plasmon band of AuNPs-HDA in CH_2Cl_2 after addition of diAOc (a) and TOABr (b) to gold nanoparticles. The inset shows TEM microphotograph of gold nanoparticles 19 h after addition of 1,8-diaminooctane

The plasmon absorption peak shifts from 525 nm to 570 nm for diAOc and to 563 nm for TOABr, upon ligand exchange. The presence of an isosbestic point on the

blue side of the absorption band (496 nm) for diAOc and at the red side (549 nm) for TOABr indicates that at the early stage of the ligand exchange at least two spectral individuals exist in the colloidal solutions. The quick formation of a second band, which progressively red-shifts while the initial band either remains unchanged (Fig. 1a) or slightly drops in intensity (Fig. 1b) accounts for the aggregation of the starting gold colloid. The observed shift of the plasmon resonance maximum is attributed to near field coupling occurring when the interparticle distance decreases [19]. The smaller the interparticle distance, the larger the red shift is. In fact, in both cases the original long aliphatic chain ligand is replaced by twice as short capping agents. The evolution of absorption bands indicates that exchange of HDA by diAOc is far slower than that of TOABr. It requires at least 15 h and 1 h, respectively, to reach a state where changes in the spectra are negligible.

The time evolution of the plasmon band shows that positively charged groups easily replace amine ligand. This is consistent with the observed trend in reactivity, which reveals that charged ligands generally require considerably shorter reaction times than uncharged ones. On the other hand, an increase in extinction for AuNPs-HDA/diAOc mixture is intriguing. The explanation is provided by a TEM micrograph (inset in Fig. 1a) which indicates that diAOc promotes a special shape of aggregates, in the form of chains consisting of 2-4 linearly ordered gold particles. Unfortunately, the aggregates are not stable enough and after few days finally precipitate from the solution. It means that, upon desorption of HDA, the steric stability of nanoparticles is disturbed and causes irreversible aggregation of colloidal nanoparticles.

3.2. Binding of disulfides and thiols to HDA-protected gold nanoparticles

High stability against aggregation of AuNPs-HDA nanoparticles was observed when amine ligand was exchanged for thiol. Thus HDA-protected gold nanoparticles enable investigations of such a reaction. For its examination, we applied a fluorescence method. As a photofunctionalized dopant for protecting monolayers, we synthesized fluorescent disulfide using commercially available pyrene. The system of HDA capped nanoparticles and the fluorophore offers the possibility to probe the binding of disulfides to nanoparticles through its fluorescence emission. The symmetric pyrene-disulfide molecule itself shows a structured monomer emission band and a distinct intramolecular excimer band in its fluorescence spectrum. This excimer band is evident even at very low concentrations and results from the fixed connection of the two pyrenyl groups.

First, we studied the binding of pyrene disulfide to the particle surface by observing the quenching of pyrene fluorescence. To the solution of diSPy (Fig. 2, curves a) in dichloromethane ([pyrene] = 3×10^{-6} M) a drop of concentrated colloid of AuNPs-HDA was added. An instantaneous fluorescence drop was observed due to an inner filter effect (Fig. 2A, dotted line). During the next few hours, a continuous diminution of fluorescence was observed, as was evidenced by a series of emission spectra

and changes in fluorescence intensity at 377 nm. Moreover, we have noticed that the excimer emission peak at 476 nm decreases faster than the monomer one.

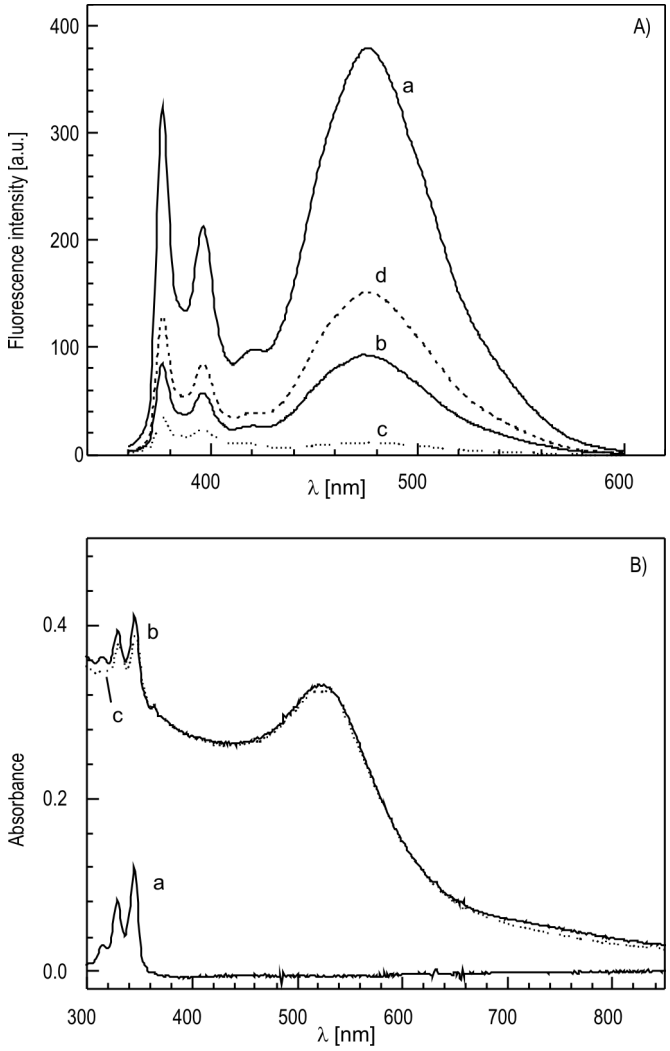

Fig. 2. Fluorescence (A) (λ_{ex} = 346 nm) and absorption (B) spectra of diSPy in dichloromethane recorded before (a) and after addition of AuNPs-HDA: b – 80 min and c – 22 h. Dashed line (d) represents the spectrum immediately upon AuNPs-HDA addition and shows dropping in fluorescence intensity due to the inner filter effect originating from the gold nanoparticles. Both monomer and broad excimer bands decrease vs. time; [pyrene] = 3×10^{-6} M

Initially the intensity ratio I_{476}/I_{377} amounts to 1.18 while after 22 h it drops to 0.33. This result suggests that the two parts of disulfide mainly adsorb independently from each other on the Au particle surface. Similar separation of disulfide moiety was noticed in the EPR study on the nitroxide diradical probe [6]. The reaction of

AuNPs-HDA with diSPy at low concentration produces a similar coverage of the gold surface as the exchange reaction with an excess of pyrene disulfide (I_{476}/I_{377} = 0.32, *vide infra*). The absorption spectrum after 1 h of reaction does not superimpose on the absorption spectra of diSPy and AuNPs-HDA nanoparticles and during the exchange reaction it red-shifts and reduces its absorbance by 1.8 times (from 0.127 to 0.071). This indicates an enhancement of interactions between pyrene moieties and the gold core.

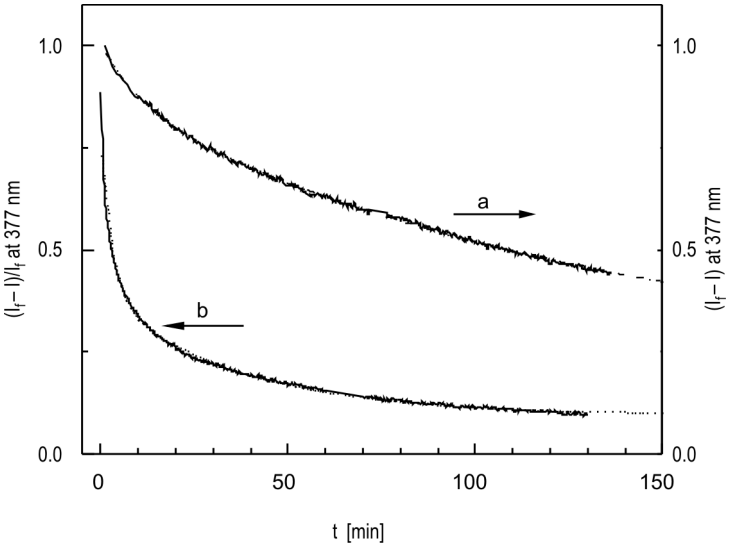

Fig. 3. Kinetics of chemisorption (a) of diSPy to AuNPs-HDA gold surface and its desorption (b) after the injection of 10^{-3} M HDT measured by changes in the fluorescence intensity at 377 nm.
The dotted lines represent fitting with two exponentials

Time dependences of changes of fluorescence intensity at 377 nm normalized to final intensity after complete binding of diSPy to the surface of the NPs are shown in Fig. 3. The exchange reaction, where amine is replaced for disulphide, involves a slow and a fast step. This behaviour can be ascribed to different spots on the NP surface. The fast step takes place at the edges or vertexes, where disulfides can reach gold quite easily. The kinetics slows down in flat domains, where molecules are tightly packed and functionalization takes more time. A similar trend in kinetic exchange processes was previously observed for flat gold substrates [20] and gold nanoparticles [8]. The monomer emission data were analyzed by a double-exponential function. The empirically determined values of characteristic decay times obtained by fitting the fluorescence intensity profiles with a sum of two exponentials

$$I(t) = A_1\exp(-t/\tau_1) + A_2\exp(-t/\tau_2)$$

upon chemisorption of diSPy and desorption of SPy from the gold nanoparticles surface are given in Table 1.

Table 1. Characteristic decay times

Observed phenomenon	τ_1 [min]	τ_2 [min]	r_2
Chemisorption of diSPy to Au core[a]	10.7±2	133.5±0.8	0.999
Desorption of SPy from Au core[a]	2.93±0.04	36.40±0.40	0.997
Desorption of SPy from Au core[b]	1.63±0.13	34.40±5.76	0.998

[a]Place exchange reaction on HDA-protected gold nanoparticles.
[b]Place exchange reaction on diSPy-protected gold nanoparticles

On the same sample, we were able to conduct an opposite experiment, namely desorption of pyrene from the gold surface. In the presence of hexadecanethiol, another exchange reaction occurs in colloidal solution, setting pyrene free from gold [8]. As a result, a recovery of fluorescence against time is observed (Fig. 4). However, only the monomeric band undergoes enhancement while the intensity of excimer emission stays at the level before the HDT injection. Two kinetic processes occur with changes in fluorescence intensity with different rates of fluorescence recovery (Table 1). Interestingly, although desorption is faster than chemisorption, there exists a relationship between the time parameters τ_1 and τ_2 for chemisorption and desorption. The ratio τ_2/τ_1 (equal to 12.4) is the same for both samples, similarly as the ratio τ_1(chemisorption) /τ_1(desorption), equal to the ratio τ_2(chemisorption)/τ_2(desorption) (amounting to 3.7).

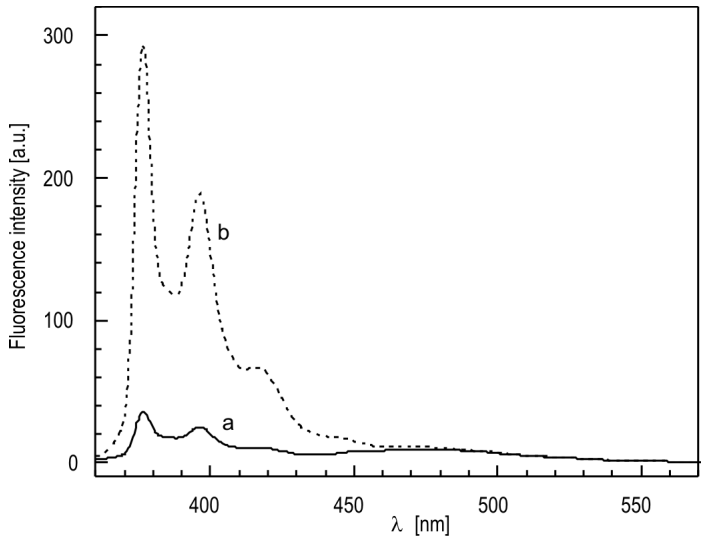

Fig. 4. Time evolution of the emission spectrum (λ_{ex} = 346 nm) of a solution of AuNPs-Py in CH_2Cl_2 (a) and after injection of HDT (b). The monomer band increases upon time whereas the excimer band remains fixed

The discussed place exchange reaction of pyrene disulfide on Au nanoparticles directly illustrates S–S bond cleavage on gold, followed by formation of Au–S bonds and finally Au–S dissociation in the presence of a stronger thiolate ligand.

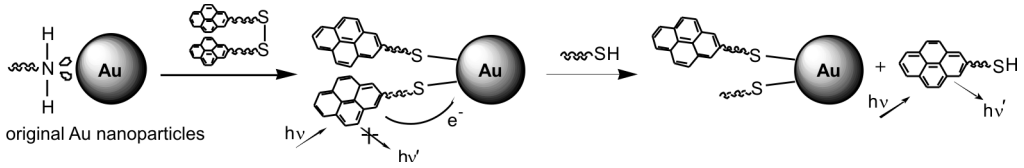

Scheme 2. Mechanism explaining the observed fluorescence from bispyrene disulfide molecules chemisorbed and desorbed from gold NPs surface

The overall mechanism of the fluorescence quenching and enhancement consistent with our observations is schematically presented in Scheme 2. The fluorescence of the pyrene probe gradually diminishes upon its binding and arrangement on the gold surface. Several mechanisms have been considered [21, 22], however for gold particles of dimensions around 10 nm and molecules having more than 4 carbon atoms in the linking chain, fluorescence quenching occurs mainly by electron transfer to the gold NP [12, 15], with the formation of a pyrene radical cation. Upon subsequent HDT addition, fast release of pyrene takes place, which is manifested by the fluorescence enhancement of gold colloid.

3.3. Place exchange reaction on diSPy-protected gold nanoparticles

Starting from purified HDA-capped gold particles in toluene, we synthesized NPs coated with a monolayer of pyrenesulfide by adding an excess of diSPy at elevated

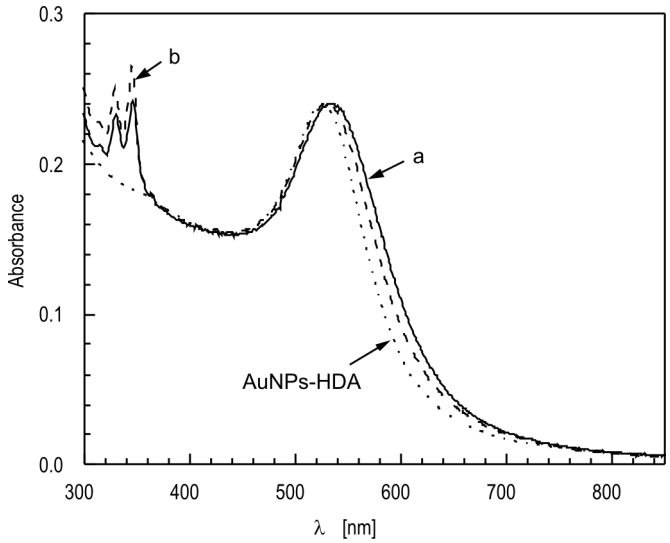

Fig. 5. UV-Vis absorption spectra of AuNPs-diSPy in dichloromethane before (a) and 80 min after (b) addition of 10^{-3} M HDT. The dotted line represents absorption of HDA-stabilized gold nanoparticles

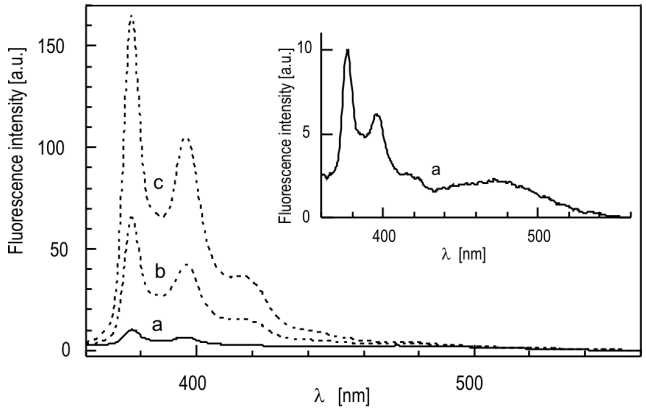

Fig. 6. Fluorescence spectra of pure AuNPs-diSPy nanoparticles (a), and 80 min (b) and 2 days (c) after addition of 10^{-3} M HDT. The inset shows the magnified fluorescence spectrum (a) of the initial colloidal solution

temperature. Such functionalized particles were purified by precipitation using ethanol. The UV-vis spectra of AuNPs-HDA and AuNPs-Py redispersed in dichloromethane are presented in Fig. 5. They display typical pyrene related peaks at 313, 328 and 346 nm, which are slightly broadened and red shifted in comparison with a free pyrene chromophore. The surface plasmon resonance absorption band of thiol-passivated gold nanoparticles has a maximum located at noticeably longer wavelength (λ_{max} = 534 nm) as compared to that of the HDA-stabilized particles (λ_{max} = 525 nm). This observation is in accordance with the presence of thiols on the gold particle surface. The fluorescence emission spectrum of AuNPs-Py shows similar excimer-to-monomer intensity ratio (I_{476}/I_{377} = 0.32), as pyrene modified nanoparticles obtained from AuNPs-HDA and diSPy at 25 ºC in CH_2Cl_2 (the inset in Fig. 6.).

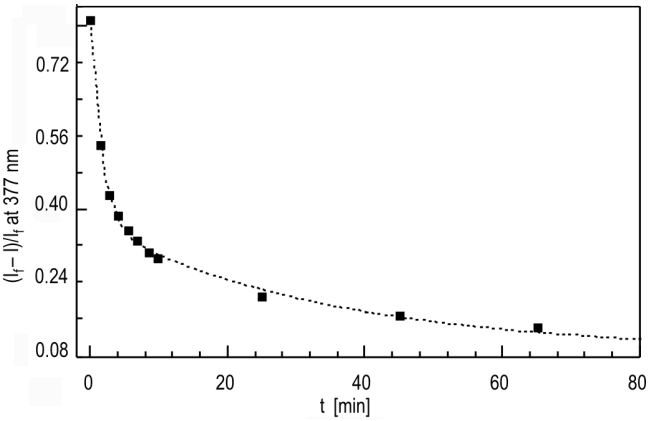

Fig. 7. Kinetics of the relative changes of fluorescence intensity at 377 nm for AuNPs-diSPy colloid after the injection of 10^{-3} M HDT. The dotted line represents fitting with two exponentials

We also attempted to verify whether sample preparation conditions influence the kinetics of ligand exchange reaction [8]. Immediately after the addition of HDT to a colloidal AuNPs-Py solution, similarly as in the previously studied system, an increase in monomer fluorescence intensity is observed. There are no accompanying changes to the intensity of the excimer (Fig. 6). While the monomer fluorescence profile keeps its shape, pyrene absorption peak blue-shifts and increases its absorbance by 1.9 times. Simultaneously the plasmon band shifts to λ_{max} = 528 nm, indicating changes in ligand–gold nanoparticle interactions. The kinetics of the ligand exchange reaction is also described by a two step process, as was discussed earlier (Fig. 7). The fast desorption process τ_1 is characterized by slightly faster kinetics, while the slow one has the same decay time τ_2 (Table 1).

4. Conclusions

We have studied place exchange reactions of aliphatic disulfides and thiols on two types of gold colloids. We were able to compare kinetic processes of binding and detachment of pyrene disulfide from a gold surface. First, starting with HDA-protected nanoparticles, we monitored the adsorption of bis-functionalized disulfides by fluorescence quenching of pyrene. After completion of the HDA for diSPy ligand exchange reaction, we studied the kinetics of diSPy for HDT replacing reaction on the same sample. The second colloid were gold nanoparticles, caped with pyrene disulfide prepared in the ligand excess at elevated temperatures. In both cases fluorescence intensity as well as absorption were significantly attenuated upon bonding to NPs as compared with the solution of free diSPy. When pyrene sulfide was displaced by HDT, the opposite effect took place as was evident from the fluorescence enhancement and absorption increase. Another observation was a fixed low efficiency excimer emission of pyrene linked to gold nanoparticles as compared to the bulk solvent. We ascribed this residual emission to a very small fraction of diSPy which may be not subject to S–S bond cleavage on gold.

In the literature, the accepted mechanism for the main deactivation channel of the singlet excited state of pyrene linked to gold with a longer spacer is electron transfer to the gold core [12, 15]. This unexpected result is ascribed to chain flexibility, enabling appropriate arrangement of pyrene moiety and interaction with gold surface. Significant changes in gold plasmon band position cannot be simply explained based on the sulphide for thiol exchange, since the interfacial sulfur and carbon atoms remain the same in both ligands. Our hypothesis is that ω-functionalized sulfides form, opposite to alkanethiolate monolayers, loosely-packed coverage enabling short-distance pyrene–gold interactions through an appropriate geometrical arrangement. This would also explain the attenuated absorbance of pyrene on gold NPs.

Acknowledgement

This work is financed by the Polish Ministry of Scientific Research and Information Technology project No. 3T08E 02228.

References

[1] BRUST M., WALKER M., BETHELL D., SCHIFFRIN D.J., WHYMAN R., Chem. Comm. (1994), 801.
[2] LEFF D.V., OHARA P.C., HEATH J.R., LANGMUIR, 12 (1996), 4723; HIRAMATSU H., OSTERLOH F.E., Chem. Mat., 16 (2004), 2509; FLEMING D.A., WILLIAMS M.E., Langmuir, 20 (2004), 3021.
[3] HOSTETLER M.J., TEMPLETON A.C., MURRAY R.W., LANGMUIR, 15 (1999), 3782; PETROSKI J., CHOU M.H., CREUTZ C., Inorg. Chem., 43 (2004), 1597.
[4] BOAL A.K., ROTELLO V.M., J. Am. Chem. Soc., 122 (2000), 734.
[5] WOEHRLE G.H., BROWN L.O., HUTCHISON J.E., J. Am. Chem. Soc., 127 (2005), 2172.
[6] IONITA P., CARAGHEORGHEOPOL A., GILBERT B.C., CHECHIK V., J. Am. Chem. Soc., 124, (2002) 9048.
[7] WERTS M.H.V., ZAIM H., BLANCHARD-DESCE M., Photochem. Photobiol. Sci., (2004), 29.
[8] MONTALTI M., PRODI L., ZACCHERONI N., BAXTER R., TEOBALDI G., ZERBETTO F., Langmuir, 19 (2003), 5172.
[9] WRIGHT A., GABALDON J., BURCKEL D.B., JIANG Y.-B., TIAN Z.R., LIU J., BRINKER C.J., FAN H., Chem.Mater., 18 (2006), 183034; UNG T., LIZ-MARZAN L.M., MULVANEY P., J. Phys. Chem. B., 105 (2001), 3441.
[10] UZNANSKI P., AMIENS A, CHAUDRET B., BRYSZEWSKA E., Polish J. Chem., 80 (2006), 1845.
[11] REYNDERS P., KUEHNLE W., ZACHARIASSE K.A., J. Phys. Chem., 94 (1990), 4073.
[12] THOMAS K.G., KAMAT P.V., Acc. Chem. Res., 36 (2003), 888; IPE B.I., THOMAS K.G., BARAZZOUK S., HOTCHANDANI S., KAMAT, P.V., J. Phys. Chem. B, 106 (2002), 18.
[13] CANEPA M., FOX M.A., WHITESELL J.K., Photochem. Photobiol Sci., (2003), 1177
[14] WANG T., ZHANG D., XU W., YANG J., HAN R., ZHU D., Langmuir, 18 (2002), 1840.
[15] BATTISTINI G., COZZI P.G., JALKANEN J.-P., MONTALTI M., PRODI L., ZACCHERONI N., ZERBETTO F., ACS Nano, 2 (2008), 77.
[16] IONITA P., VOLKOV A., JESCHKE G., CHECHIK V., Anal. Chem., 80 (2008), 95.
[17] BARDAJI M., UZNANSKI P., ANIENS C., CHAUDRET B., LAGUNA A., Chem. Comm. (2002), 598.
[18] DRABOWICZ J., MIKOŁAJCZYK M., Synthesis, (1980), 32.
[19] MULVANEY P., Langmuir, 12 (1996), 788.
[20] LOVE J.C., ESTROFF L.A., KRIEBEL J.K., NUZZO R.G., WHITESIDES G.M., Chem. Rev., 105 (2005), 1103.
[21] DULKEITH E., RINGLER M., KLAR, T.A., FELDMANN, J., MUÑOZ, JAVIER A., PARAK W.J., Nano Lett., 5 (2005), 585.
[22] YUN C.S., JAVIER A., JENNINGS T., FISHER M., HIRA S., PETERSON S., HOPKINS, B.; REICC N.O., STROUSE, G.F., J. Am. Chem. Soc., 127 (2005), 3115.

Received 13 July 2008
Revised 26 September 2008